Simulation and Modeling of Eddy Current Brakes for Hyperloop

Alex Seligson, Sam Shersher, Dan Kim, Mark Koszikowski, and Jacques Mosseri
The Cooper Hyperloop *

Eddy currents are unique electromagnetic phenomena that occur when a changing magnetic flux induces an electric field in a conductive surface according to Faraday's and Ohm's laws. Eddy currents have been harnessed to create contactless Eddy Current Brakes (ECB's) for large vehicles and more recently for Hyperloop pods. The main benefits of eddy current braking as opposed to traditional friction braking is a dramatic decrease in wear and a braking force that increases with speed. This paper uses Finite Element Analysis (FEA) and analytical models as techniques to obtain the braking characteristics of an ECB design. It is found that the presence of a back iron in the ECB and the length of the air gap both strongly effect the braking force. Different configurations of permanent magnets are also discussed. These design considerations and techniques can help Hyperloop teams create lightweight but powerful and safe ECB's in the future.

I. INTRODUCTION

Hyperloop is a method of high-speed transportation first put forward in 2013 in a Tesla whitepaper entitled "Hyperloop Alpha" [1]. The design features small segments called "pods" that travel through an evacuated tube. The two main challenges to high speed terrestrial transportation – air resistance and friction – are addressed with a vacuum and air bearings, respectively. The air bearings serve as a lower-cost alternative to electromagnetic suspension as a levitation mechanism, freeing the pod from the speed limits associated with wheels. One challenge that arises naturally in levitating trains is braking, since conventional braking systems rely on friction. There have been many designs put forward to replaced friction braking and eddy current braking (ECB) look like one of the more promising methods especially because it has been proven in other modes of transportation such as trains.[2]

Eddy currents arise when a changing magnetic field passes through a conductive object. These currents flow in closed loops within the conductive material and, according to Faraday's law, these currents create their own magnetic field which opposes the original magnetic field. The magnetic flux in a surface is defined by the amount of the magnetic field passing through that particular surface. Since eddy currents are generated from changing magnetic fields, they depend heavily on the amount and change in flux. Faraday's law, one of the Maxwell equations, is critical in how the eddy current phenomena arises. For a coil of wire with N turns, Faraday's law of inductions states that

$$\varepsilon = -N\frac{d\phi}{dt} \tag{1}$$

where ϵ is the electromagnetic force, N is the number of turns and ϕ is the flux. The more general form Faraday's law applicable to eddy current braking is

$$\nabla \times \vec{E} = -\frac{d\vec{B}}{dt} \tag{2}$$

This equation gives us a relationship between a time-varying magnetic field, $\vec{B}$, and a spatially varying electric field, $\vec{E}$. Based on this equation, when a magnet passes by a conductive material, the edges of the magnet cause a change in magnetic field from the perspective of the conductor and thus the eddy current phenomena arises. A classic example of this phenomenon is a magnet falling down a copper tube. The magnet falls at a constant and slow rate due to the opposing forces produced by the eddy currents in the tube, like an object in free fall at terminal velocity. This is because in this situation, the Lorentz force, like the drag force, is roughly proportional to speed. Much of the potential energy of the magnet at the top of the tube is converted to heat dissipated by the tube's finite resistance. Therefore, these forces can be calculated quite easily by finding the induced currents in each circular cross section and integrating to find the total power dissipation due to ohmic losses. The force can then be found easily from the power since the magnet is moving at a constant speed. This retarding force can be harnessed in breaks for Hyperloop pods. Much of the literature on ECB's in vehicles discusses circular eddy current brake systems with a permanent magnet or coil held around a conducting wheel, but for trains or Hyperloop pods operating on aluminum tracks, a linear eddy current brake system is more convenient. The linear system offers less heating since the induced current effects a different part of the track every second - unlike the rotating design, the same part of the track is never "reused" by the brake. Both forms of eddy brake systems offer the advantage of being contactless. This reduces the excessive wear and heat dissipation caused by friction breaks, allowing the eddy current break to operate at much faster speeds. This is ideal for potential high-speed transportation systems like Hyperloop.

* TheCooperHyperloop@gmail.com

II. METHODS

1. Level Zero Model

Calculating the magnetic drag force directly from ohmic losses proves difficult or even impossible in general. This is because in most geometries, induced eddy currents follow complicated paths so that there are no well-defined current loops. This makes it impossible to use a circuit model to calculate ohmic losses like in the magnet-in-tube example. [3]. Therefore, the current density at each point in the conductor is typically used instead of the current, and the Lorentz force becomes $\vec{J}\times\vec{B}$. As long as the magnetic field is known, this force acts at each point in space and can be integrated through the volume of the conductor to find the total drag force.

A "Level Zero" model was used to understand the braking force at various speeds for a single magnet. Equations from "Magnetic braking: Improved theory" by Mark A. Heald were adapted to fit the needs of the Hyperloop braking system. Three key assumptions were made during setup: (1) the magnet had a constant magnetic field, (2) there was no airgap between the magnet and the rail, and (3) that $J = 0$ if not along skin depth. Without an airgap, the B field can be assumed normal to the velocity at every point. This turns the cross products involved into simple multiplication.

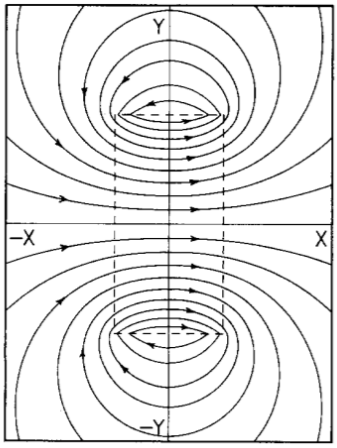

FIG. 1: Bird's eye view of the single magnet or "level zero" model. The dashed line is the outline or "footprint" of the magnet and contours shown are eddy currents induced in the plate. The magnet is traveling in the +y direction [4]

To calculate the braking force, the current density, J, was found using the E-field version of Ohm's law.

$$\vec{J} = \sigma(\vec{E} + \vec{v}\times\vec{B}) \tag{3}$$

where σ is the electrical conductivity, E is the electric flux density, v is the velocity and B is the magnetic flux density.

By incorporating the geometry of the problem (Fig. 1), one can find the resulting braking force (Eqn 4)

$$\vec{F} = \int \vec{J}\times\vec{B_0}d\tau = -\sigma\delta B_0\int_{-a}^{a}\int_{-b}^{b}(E_x + vB_0)dxdy\hat{j}$$

$$= -\alpha(\sigma\delta(B_0)^2 lw)v\hat{j} \tag{4}$$

Where F is the braking force, σ is the conductivity, α is a geometric scaling factor dependent on the aspect ratio of the magnet (calculated using equation 5), δ is the skin depth (calculated using equation 8), $\vec{B_0}$ is the magnetic field, l is the length of the magnet, w is the width of the magnet and v is the velocity of the magnet relative to the plate. Instead of the skin depth the track thickness was substituted in the above equation as the skin depth is much larger for the speeds considered. α is calculated as

$$\alpha = 1 - \frac{1}{2\pi}[4\tan^{-1}A + A\ln(1+\frac{1}{A^2}) - A\ln(1+A^2)] \tag{5}$$

where $A = \frac{l}{w}$ is the aspect ratio of the magnet footprint.

In this model, braking force acts as a drag force and has a linear relationship with velocity. In order to improve this example and to get a more realistic approximation of the braking force, a variable magnetic field and an air gap are required.

2. Array Model

Magnetic arrays are typically used instead of single magnets to maximize the change in magnetic flux and therefore the total drag force. These arrays alternate in polarity so that the magnetization of the array is a periodic function and can be easily modeled using harmonic analysis. [5] Another common element in permanent magnet linear ECB designs is a backiron, or a slab of high-permeability soft magnetic material. This reduces the total reluctance, or resistance to magnetic flux, of any given flux path produced by the permanent magnet array. A diagram of a typical magnetic array design with a backiron is shown in figure 2.

A frequency can be defined as $\beta = \frac{\pi}{p}$ where p is the pole pitch (i.e. width of a pole) and is based on the "wavelength" of the array and its velocity. This means that it is a time dependent harmonic problem —greatly simplifying both the analytical solutions and the finite element simulations. In Finite Element Analysis (FEA), each added dimension or independent variable increases the necessary computation exponentially. Therefore, for a harmonic problem with a dominant fundamental frequency component it often makes more sense to work the phasor domain than in the time domain. For this reason, FEMM, a popular and simple magnetics solver used

in this paper, has the capability to solve time-harmonic problems but not problems in the time domain.

The main partial differential equation (PDE) of importance in time-harmonic eddy current problems is the Helmholtz equation [6]. In eddy current problems, the nonhomogeneous vector Helmholtz equation can be easily derived to describe the B field. First, the B field can be broken into 2 parts, the external field, generated by the permanent magnets, and the induced field, generated by the eddy currents. Using Maxwell's equations and the assumption that all fields involved are complex spatial exponentials, one can find the PDE

$$\nabla^2 \vec{B_e} + k^2 \vec{B_e} = -k^2 \vec{B_i} \tag{6}$$

Where $\vec{B_i}$ is the B field from the magnets and $\vec{B_e}$ is the B field created by the eddy currents. Assuming the spatial components of the solution are separable, the solutions of this equation are sums of complex and decaying exponentials. Once $\vec{B_e}$ is solved for, the current density and therefore the Lorentz force can be easily calculated since $\vec{J} = \nabla \times \vec{B_e}$.

This formulation is convenient to use in general purpose FEA solvers like Deal ii when B is already known. However, the non-constant forcing condition on the right hand makes finding an analytical solution very difficult. Therefore, the Helmholtz equation for eddy currents is usually written in terms of the vector potential, or A field instead. This equation takes the form:

$$\nabla^2 \vec{A} + k^2 \vec{A} = 0 \tag{7}$$

[7]

3. Analytical Model

Because of the periodic nature of this setup, the theory of AC circuits can be used to get a general form for the drag force [12]. The form of the drag force is:

$$F_D = \frac{A'v}{v^2 + B'} \tag{8}$$

with A' and B' as constants that are treated as parameters. B must be a positive constant. This model is fitted to the simulation results using Matlab's cftool add-on. It is convenient to have a simple model for the force as a function of speed because then the force can be quickly calculated by the pod at any time during flight.

One major difference between this model and the previous linear model for one magnet is the "compensation speed", the speed at which the force reaches a maximum. The maximum braking force is similar in principle to the pull-out torque of an induction motor, the maximum torque after which the motor will stall. [8]

4. Halbach Arrays

As can be seen clearly in the level zero equations, the maximum braking force depends primarily on the amount of magnetic flux penetrating the track. This remains true for more complicated models. Therefore, the main design goal of the ECB is to maximize the flux for a given assembly mass. One way to increase the magnetic field is simply to buy stronger magnets. Besides this, magnetic arrays can be configured in clever ways that localize the magnetic field on one side of the array.

The Halbach array is an array that has a large magnetic field on one side and a very small magnetic field on the other side (Fig. 7). Another added benefit of using Halbach arrays is the "shielding effect" of Halbach arrays. An alternating magnetic array has two effective sides of equal and opposite strength while a Halbach array only has one. For an alternating setup there is an equal magnetomotive force (MMF) drop on both sides because the flux is shared equally on both sides. On the other hand, Halbach arrays only have one effective side, so most of the magnetic flux travels back through the magnet and leaves the strong side, never escaping the weak side of the magnet. This means that, unlike alternating arrays, Halbach arrays do not need a back iron for the flux to return. This is particularly useful for Hyperloop because this reduces the mass of the braking system and increases the effectiveness of the brakes. The literature has shown that Halbach arrays have a stronger flux density on the strong side than alternating pole arrays and result in stronger induced eddy currents. [5]

The main drawback to Halbach arrays is the difficulty of constructing them. The magnets must be forced together in spite of strong torques and forces pushing them apart. The side profile of the magnets must also be square due to the geometry of the array.

Halbach arrays can be modeled in FEMM as permanent magnets with great ease. The magnetization direction of a region can be directly specified, and it can easily be rotated by 90 degrees between regions.

A. Software

In order to theoretically evaluate the magnitude of the eddy braking force for different geometries, it was decided to build the model using a multiphysics software in order to run simulations that would model the braking force. The software packages considered were COMSOL, ANSYS Maxwell, Deal II and FEMM. COMSOL is an extensive multiphysics software that can run 3-D, time domain and frequency domain simulations with multiple physical systems. The package needed to run simulations on permanent magnets is the ACDC Module, access to which was unavailable at the time needed. It was then chosen to build the model in FEMM due to the team's familiarity, its simplicity and ease of access, and its wealth of documentation.

FEMM can be accessed through MATLAB or a built in Graphical User Interface (GUI). The Matlab interface makes it easy to programmatically run simulations with different geometries. In the paper "Analysis of an Eddy Current Brake with FEMM" by David Meeker, the braking force of an alternating pole magnet array (Figure 1) is calculated using the Matlab interface to FEMM [9]. In the model, a one-sided array of permanent magnets moves along a conductive surface, separated by a thin air gap. In the context of linear induction motors, this design is commonly referred to as a "long stator" design.

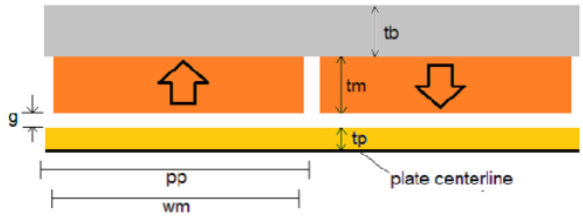

FIG. 2: Cross-section of the assembly used in the braking force simulations. The grey area is the backiron, the orange rectangles are magnets that are magnetized as indicated, and the yellow region is the conducting track.This figure was taken from source [9]

The simulations use only one wavelength of the geometry – that is, two pole pitches or two magnets – but use periodic boundary conditions to capture the effects of a long array. Therefore, the forces obtained can be scaled to the actual size of an array without losing much accuracy. Only rough corrections for end effects are made. The paper chooses to model the magnetic array as current sheets perpendicular to the array since the equivalent-current model is required in FEMM for time-harmonic problems. The fundamental frequency of the alternating current sheets can then be used to specify the source currents in the magnets.

The dimensions of the array, strength of the magnets and the gap length were changed slightly from the original code to more accurately reflect a potential ECB design for Hyperloop. In particular, the conductivity of the conductor was changed to that of Aluminum 6061 (the material of the Hyperloop track) and specifications of the magnets were replaced by those of the magnets used in the 2019 Cooper Union Hyperloop design. Additionally, in the original code the periodic current density function that was used to model the permanent magnets had to be discretized into sections with constant J. The number of these sections was increased for further accuracy.

The equivalent-current permanent magnet model works well for the alternating poles array, but it breaks down when modeling a Halbach array. Modeling a Halbach array as current sheets, or solenoids, requires odd numbered solenoids to be turned on their side, breaking the periodicity of the problem. [10] If an alternating current sheet is instituted in the vertical direction in FEMM so as to produce a horizontal magnetization, the magnetic field does not behave like a Halbach array should. Additionally, due to the non-harmonic and 3D implications, FEMM also cannot model edge effects or variations of B in the depth dimension. Despite these limitations, FEMM was a convenient starting point for simulating the effects of a backiron and different gap lengths on the braking force.

III. OTHER CONSIDERATIONS

Skin depth was also a potential consideration because it could limit the induced eddy currents. This could be a problem, because if the skin depth is too small, then the braking force will be dramatically reduced. At faster speeds (and therefore higher frequencies), the eddy currents weaken in the depth dimension so that most of the current density is localized to the surface of the track. Skin depth is the measure of how localized the currents are at high frequencies. The general equation for skin depth is

$$\delta = \frac{1}{\sqrt{\pi f \mu \sigma}} \tag{9}$$

Where δ is the penetration depth (m), f is the frequency (Hz), μ is the magnetic permeability (H/m) and σ is the electrical conductivity (S/m).

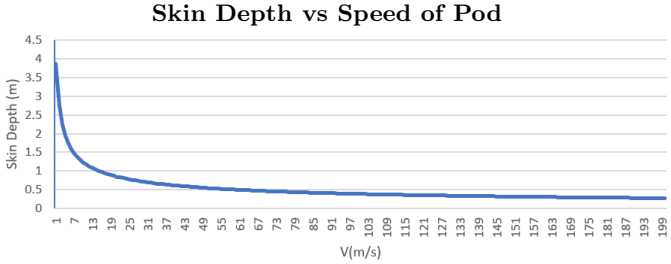

FIG. 3: The skin depth for speeds up to 200 m/s (447 mph). Even for these fast speeds, the skin depth is much larger than the scale of the problem and can be ignored.

Figure 3 is a graph of equation 8, showing the relationship of skin depth to speed. The lowest value of skin depth is 0.27 m at 200 m/s (447 mph). Since the thickness of the track is under 0.1 m, and the record for fastest pod speed is 129 m/s, the varying skin depth penetration should not affect the braking force.

The current design of the Cooper Union Hyperloop team employs Neodymium magnets. These magnets are fairly linear so the linear (constant μ_r) approximation such as the one made by FEMM should not reduce accuracy by much. This is good because a problem with a non-constant μ_r is non-linear and hysteretic, making it very difficult to solve.

End effects, or the reduction in braking force due to the finite length of the array, are also ignored in the above model.

IV. RESULTS

1. Level Zero Results

The "Level Zero" Model evaluates the braking force of a single magnet. In this rough model, the braking force is linearly dependent on the velocity (fig 4). In more detailed models this is not the case and there is a rational polynomial relationship instead, as discussed in the analytical model.

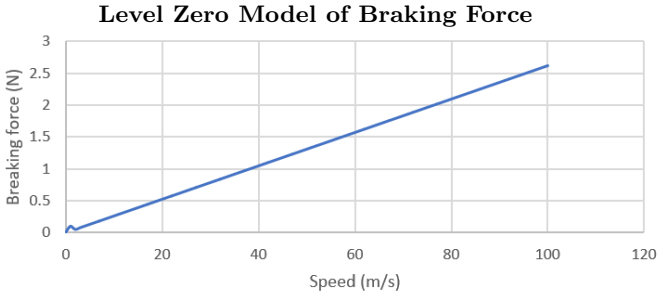

FIG. 4: Simple linear model relating braking force to speed for a single magnet.

2. FEMM Results

The FEMM simulations were performed at rest and at speeds up to 100m/s, with the speeds stepping up by 4 m/s between simulations. The 2-parameter model for drag force presented earlier was used to fit the datapoints.

Tests were conducted with and without the backiron. In the simulation without a backiron, the steel region was replaced with air. The results of these two simulations are shown in Fig. 5.

Simulations were then performed with a backiron and air gap lengths ranging from 1 mm to 5 mm. The resulting data points and fitted curves are shown in Fig. 6.

As discussed earlier, Halbach arrays concentrate most of the flux on one side. FEMM simulations were used to compare Halbach arrays to alternating arrays with and without a backiron. The $\vec{B}$ field diagrams for all three cases are shown in Fig. 7 with the number of flux lines normalized.

V. DISCUSSION

The level zero model predicts a braking force for a single magnet an order of magnitude below that predicted

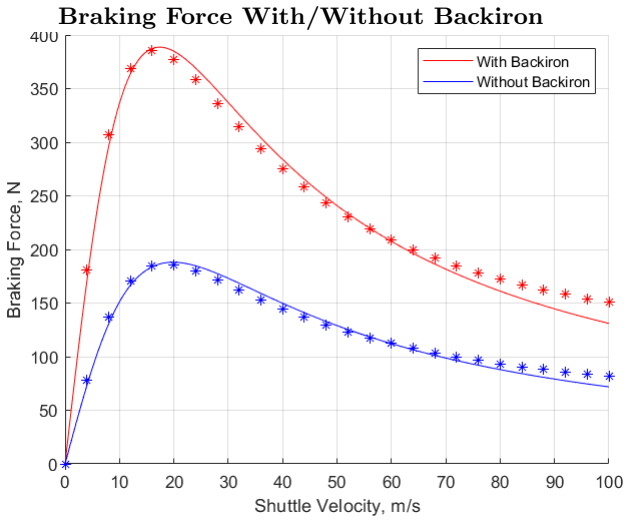

FIG. 5: Braking force as a function of speed with and without a backiron. The datapoints are obtained from a FEMM simulation and the curves are equation (8) fitted to the data.

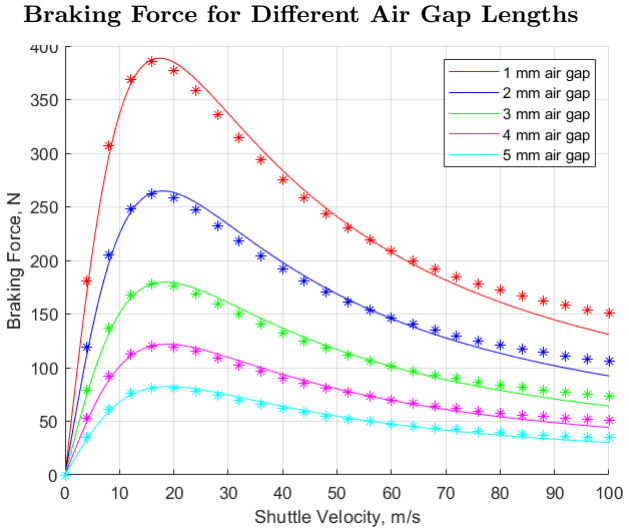

FIG. 6: Braking force as a function of speed for five different air gap lengths, ranging from 1-5 mm

by the FEMM simulation. One reason for this, besides the simplicity of the linear model, is that the addition of multiple poles as can be found in an array greatly increases the right hand side of equation (2), thus increasing the induced EMF in the track. Because of the level zero model's vast under prediction of the braking force when scaled up to an array, it is not a good model even for simple hand calculations of eddy braking force curves. A better way to estimate the force from an array without simulation or experimental data to use 1-D linear induction motor theory to find the expected maximum of the force curve as is done in [9].

As shown in the Figs. 5 and 6, both the size of the air

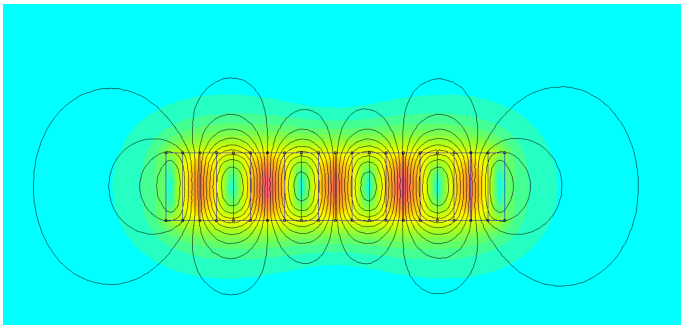

(a) Alternating polarity array without Backiron

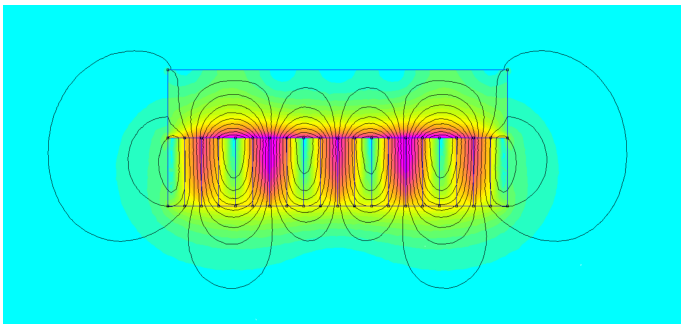

(b) Alternating polarity array with Backiron

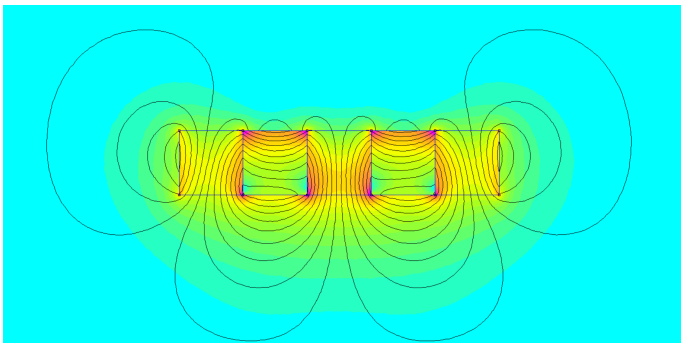

(c) Halbach Array

FIG. 7: $\vec{B}$ field lines produced by 5 poles of (a) an alternating polarity magnetic array without a backiron, (b) with a backiron and (c) a Halbach array. Purple regions have the highest $\vec{B}$ field while light blue regions have the lowest.

gap and the presence of the backiron strongly effect the maximum braking force. This is because both decreasing the air gap and the adding a backiron result in a reduction of the average reluctance to the flux paths around the array. This means that for a given external $\vec{B}$ field, more flux is produced. On the other hand, a larger air gap and the absence of a backiron result in less flux penetrating the conductor, and therefore less braking force.

The close fit of the model to the simulation data validates the simulation results. The curves obtained bear similarities the torque-slip curves of an induction motor. This is because of the increasing reactance of the assembly with speed, as can be seen in the derivation of the model in the appendix. The peak force occurs at a speed of around 16 m/s in all the simulations, a fact that arises from the mechanical frequency of the array and the conductivity of the track. [9] Since the material of the track is set at Aluminum 6061 and therefore the conductivity cannot be changed, this suggests that the speed at which the peak force occurs may be tuned by using narrower or wider magnets.

The B-field simulations confirm the literature on Halbach arrays. The field for Halbach arrays is clearly more concentrated on one side. The $\vec{B}$ field lines make it further away on the strong side of the Halbach array than on the same side of the alternating arrays. It is more intense on the strong side as the green and yellow regions in extend further from the magnet as seen in Fig. 7 (c). The addition of a backiron also increases the total flux in an alternating array as expected. The backiron case has the strongest $\vec{B}$ field intensity inside the magnet and steel by far, but only the B field below the array is useful for eddy braking. Therefore the Halbach array is the best choice neglecting factors such as ease of construction.

VI. FUTURE WORK

It is recommended that more research be done on software such as COMSOL and ANSYS Maxwell, Deal ii and FEniCS. During the course of the study the research team was unable to get access to the COMSOL and ANSYS packages due to the expensive nature of the software. Attempts were made to make use of Deal ii, but the high learning curve and overhead of the software was prohibitive. On the other hand, Deal ii is free and open source, very well documented, and code has already been written to solve the Helmholtz equation. [11] FEniCS might also be a promising choice for a PDE solver since it is written in python and has a higher level interface than Deal ii. The authors plan to investigate this software's viability in the future. Whichever software is chosen, using more sophisticated software than FEMM would allow simulations to be done in 3D and with more complicated geometries such as Halbach arrays. There is also accuracy to be gained by simulating an inherently 3D problem in 3D. After more accurate simulations are done, the next step is to do physical tests. Luckily, a test rig was set up during the 2018-2019 Hyperloop season. The experimental results will then be fitted to the same model used to fit the simulation results.

VII. CONCLUSION

In the demanding environment of the Hyperloop competition, eddy current breaks need to be be as light

weight and powerful as possible. Optimizing the design in such a way requires understanding of the many factors at play, including material properties, magnetic strength and problem geometry. The key factor to maximizing the braking force of the ECB is the magnetic flux. Using FEMM simulations, the Halbach array has been shown to produce a stronger $\vec{B}$ field and therefore more flux than an alternating array. This suggests that a Halbach array will be a more efficient orientation of magnets for this application. If an alternating pattern of magnets must be used, simulation results indicate that the addition of a backiron seriously improves performance. Increasing the air gap dramatically decreases the braking force, so the air gap should as tight as tolerances allow. In order to create the best braking system, one should strive to minimize the air gap, and maximize the change in magnetic flux however possible whether it be by changing the magnetic array or by getting stronger magnets.

ACKNOWLEDGMENTS

Thank you to Professor Philip Yecko for advising and guiding us in every step of our research.

Appendix A: Force Model Derivation [12]

The array and conductor can be modelled as an RL circuit where the voltage source is the emf around the entire surface of the conducting track: [6]

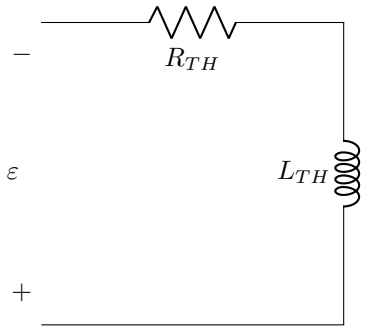

Where ε equals the change in flux across the whole track or $\frac{d}{dt}\int_S \vec{B}\cdot d\vec{S}$ and R_{TH}, L_{TH} are some unknown Thevenin equivalent resistance and inductance. It should be stressed that the impedance of the circuit cannot be calculated or measured empirically, it is just useful in deriving the forms of the force equations.

Just like in the magnet-in-tube example, the strategy is to find the total current in terms of constants and calculate the I^2R losses to find the form for the force. The total current induced in the conductor has the form

$$I_{rms} = \frac{\varepsilon}{\sqrt{R_{TH}^2 + (2\pi f L_{TH})^2}} \tag{A1}$$

The frequency f and the EMF are both proportional to the speed, so this can be rewritten as

$$= \frac{Av}{\sqrt{R_{TH}^2 + Bv^2}} \tag{A2}$$

where A and B are proportionality constants since $\varepsilon, f \propto v$. The real or true power in this circuit corresponds to the drag force - the component of the force opposite the velocity - since this is the component that does work on the pod. The power can be found by

$$P = I_{rms}^2 R = \frac{A'v^2}{v^2 + B'} \tag{A3}$$

Therefore the drag force is

$$F_D = \frac{P}{v} = \frac{A'v}{v^2 + B'} \tag{A4}$$

for some real constants A', B' where $B' \geq 0$. These constants are the two parameters used to fit the model in Matlab. The reactive power in the circuit corresponds to the lift or normal force, since this force is perpendicular to the motion of the magnetic array and therefore does no work on it. The normal force is

$$F_N = \frac{Cv^2}{v^2 + D} \tag{A5}$$

for constants C, D where $C \geq 0$.

The normal force is an important consideration, both for levitation and stability. If levitation and not braking is the main priority, the ECB-track assembly can be designed with a high inductance to get more lift. On the other hand, strong and imbalanced normal forces might require a dynamic system to maintain stability.

Appendix B: Vector Helmholtz Equation Derivation

The magnetic vector potential A is defined as:

$$\vec{B} = \nabla \times \vec{A} \tag{B1}$$

One can see how solving for A is more convenient for 2-D solvers like FEMM since the PDE gets reduced to one dimension.

This is used in conjunction with Gauss' law and Faraday's law to get

$$\nabla \times \vec{E} = -\frac{\partial \vec{B}}{\partial t} \tag{B2}$$

Faraday-maxwell equation

$$\nabla \cdot \vec{B} = 0 \tag{B3}$$

Gauss' law

$$\nabla \times (\vec{E} + j\omega\vec{A}) = 0 \tag{B4}$$

Resultant equation

This form of an equation implies there exist some ϕ such that:

$$\vec{E} + j\omega\vec{A} = -\nabla\phi \tag{B5}$$

Now using Ampere's law which states that

$$\nabla \times \vec{B} = \mu_0\vec{J} \tag{B6}$$

We can substitute (C1) in for B and get that

$$-\nabla^2\vec{A} + \nabla(\nabla \cdot \vec{A}) = \mu_0\vec{J} \tag{B7}$$

Using vector identities.
Applying Ohm's law which says

$$\vec{J} = \sigma\vec{E} \tag{B8}$$

to (B5) to results in the equation:

$$\nabla^2\vec{A} + k^2\vec{A} = \nabla(\nabla \cdot \vec{A} + \mu_0\sigma\phi) \tag{B9}$$

In order to get a unique solution for A, a solution for its divergence must be specified. Choosing

$$\nabla \cdot \vec{A} = -\mu_0\sigma\phi \tag{B10}$$

turns the right-hand side of the equation to zero resulting in a familiar Helmholtz equation form. Software packages such as Deal II are fully equipped to be able to solve a classical Helmholtz problem so this choice of the divergence of A is useful in that regard. [7]

[1] E. Musk, *Hyperloop Alpha* (2013).
[2] T. Forrister, *How Eddy Current Braking Technology Is Freeing Us from Friction* (2019).
[3] Y. Levin, F. L. D. Silveira, and F. B. Rizzato, Electromagnetic braking: A simple quantitative model, American Journal of Physics **74**, 815–817 (2006).
[4] M. A. Heald, Magnetic braking: Improved theory, American Journal of Physics **56**, 521–522 (1988).
[5] S.-M. Jang and S.-H. Lee, Comparison of three types of permanent magnet linear eddy-current brakes according to magnetization pattern, IEEE Transactions on Magnetics **39**, 3004–3006 (2003).
[6] E. Weisstein, *Helmholtz Differential Equation–Cartesian Coordinates*, from MathWorld - a Wolfram web resource.
[7] J. R. Nagel, Induced eddy currents in simple conductive geometries: Mathematical formalism describes the excitation of electrical eddy currents in a time-varying magnetic field, IEEE Antennas and Propagation Magazine **60**, 81–88 (2018).
[8] Taken from the UCalgary site on electric machines. `https://people.ucalgary.ca/~aknigh/electrical_machines/induction/im_trq_speed.html`.
[9] D. Meeker, *Analysis of an Eddy Current Brake with FEMM* (2013).
[10] M.-S. Sim and J.-S. Ro, Semi-analytical modeling and analysis of halbach array, Energies **13**, 1252 (2020).
[11] M. Allmaras, *The Step-29 Tutorial Program*, `https://www.dealii.org/current/doxygen/deal.II/step_29.html`.
[12] J. Íñiguez and V. Raposo, Numerical simulation of a simple low-speed model for an electrodynamic levitation system based on a halbach magnet array, Journal of Magnetism and Magnetic Materials **322**, 1673–1676 (2010).